ADIPEC 2024

SPE-221853-MS

Protecting HSE: Monitoring Pipe Bending Stress Using Temperature Compensated Distributed Fiber-optic Strain Sensor for Enhancing Pipeline Integrity Situational Awareness

Lufan Zou, and Omur Sezerman, OZ Optics Limited

ABSTRACT

A distributed fiber-optic strain and temperature sensor (DSTS) with less than 1mW (Laser Class 1M) of pump power has been developed by controlling depletion of pump beam resulting from coherent interaction of probe and depleted pump (CIPDP). DSTS with CIPDP technique ensures flat-noise-floor over entire fiber length, which offers same resolution and accuracy over entire fiber length and makes simultaneous measurement of strain and temperature possible. Bending stress monitoring of an 11km pipeline located in northern Alberta, Canada using temperature compensated distributed fiber-optic strain sensor with CIPDP technique is presented. The results showed that some parts of the pipeline experienced 3,063με during winter from November 2022 when the pipeline was installed to April 2023 when the soil was still frozen. The pipeline leaks due to the ambient temperature change are presented also. The leak volume of 2.187gal with the injection pressure of 105psi and the temperature difference of 39°F (21.6°C) between the line temperature and the soil temperature has been detected in one minute after a leak occurred through 1/8" orifice. All leaks with different volumes controlled by injection pressure, orifice, line temperature, and duration have been detected successfully.

1. Introduction

Pipeline integrity and disturbance are generally not monitored due to the lack of any reliable and durable techniques [1]. If a pipeline has a problem, such as cracking, corrosion, tampering, etc., it is usually realized when the output flow is affected or a severe impact has been made on the surrounding environment. No information is available in terms of the type and location of the fault. Obviously, this is an inefficient and potentially costly situation. For example, on Dec. 7th, 2022 because of combination of factors including bending stress on the pipe and a weld flaw, the 622,000-barrel-per-day (bpd) pipeline was shut after it spilled 12,937-barrels-oil in rural Kansas, Washington, USA, which was expecting $480 million remediation cost related to the incident [2, 3]. Bending stress on pipes poses a threat to pipeline integrity as it can cause excessive pipe strain, pipe buckling, and severe pipe wall deformation.

Temperature and/or strain measurements with a distributed Brillouin scattering-based sensor system provide excellent opportunity for the health monitoring of industries structures [4]. One class of Brillouin-based sensors is based on the Brillouin loss technique, whereby two counter-propagating laser beams, a pulse and a constant wavelength (cw), exchange energy through an induced acoustic field. When the beat frequency of the laser beams equals the acoustic (Brillouin) frequency, ν_B, the pulsed beam experiences maximum amplification from the cw beam. By measuring the depleted cw beam and scanning the beat frequency of the two lasers, a Brillouin loss spectrum centered about the Brillouin frequency is obtained. The sensing capability of Brillouin scattering arises from the dependence of the Brillouin frequency, ν_B, on the local acoustic velocity and refractive index in glass, which has a linear temperature and strain dependence through [5, 6]

$$\nu_B(T_0, \varepsilon) = C_\varepsilon(\varepsilon - \varepsilon_0) + \nu_{B0}(T_0, \varepsilon_0) \quad (1)$$

$$\nu_B(T, \varepsilon_0) = C_T(T - T_0) + \nu_{B0}(T_0, \varepsilon_0) \quad (2)$$

where C_ε and C_T are the strain and temperature coefficients, and ε_0 and T_0 are the strain and temperature corresponding to a reference Brillouin frequency ν_{B0}. Spatial information along the length of the fiber can be obtained through optical time domain analysis by

measuring propagation times for light pulses traveling in the fiber. This allows continuous distributions of the strain and temperature to be monitored. The spatial resolution can be varied according to the application required, even after the fibers have been installed in the structures, by simply altering the length of the light pulse used. These systems offer unmatched flexibility of measurement locations and the ability to monitor a virtually unlimited number of locations simultaneously.

From Eqs. 1 and 2, it can be concluded that to have accurate measurement of Brillouin spectra is essential to get high accuracy of temperature and/or strain and short pulse duration must be used to have high spatial resolution. It is common sense that the energy inside the short pulse in time domain will spread wide spectrum in frequency domain that causes inaccurate measurement of Brillouin spectra, which results in inaccurate measurement of temperature and/or strain. To get high spatial resolution and high accurate measurement of temperature and/or strain, one of the authors [4] demonstrated theoretically and experimentally that the Brillouin interaction of probe and pump beams in the fiber includes both pump–dc and pump–pulse interactions in the probe-pump Brillouin sensor system. The dc component can be separated into two portions by their phases after propagating through the EOM. The dc part outside the pulse length interacting with the pump gathers information from all over the fibers and loses the spatial information, whereas the interaction of the pump with the dc component inside the pulse length is coherent with the pump–pulse interaction, which amplifies the Brillouin signal significantly. It allows the probe-pump-based Brillouin sensor to detect centimeter cracks.

On the other hand, to extend sensing range is another challenge for Brillouin sensor, since the longer length fiber is, the higher attenuation and worse SNR will be. Brillouin sensor based on Brillouin loss could offer longer sensing range than that based on Brillouin gain, because the pulsed beam is amplified at the expense of the cw pump beam and the intensity of the cw pump beam will be reduced as a result of the Brillouin interaction for 32-km fiber with the maximum launched cw pump power of 10 mW [7]. The setup used for the study of Brillouin slow light [8] was similar to a Brillouin sensor system based on the Brillouin loss [9]. To get more pulse time delay a strong cw pump with tens kilometer long fiber and a weak pulse were used because of Brillouin gain based on gain parameter $G=g_B I_p L$, where g_B and I_p are the Brillouin gain coefficient and the pump power intensity in a fiber of length L. When the cw pump power is too strong, it is reasonable to neglect the cw pump depletion, which reduces the available resolution Brillouin sensor based on Brillouin loss. However, for Brillouin sensor based on the Brillouin loss technique the cw pump depletion cannot be neglected owing to the strong interaction of the weak pump and the strong probe [4, 9]. In fact, coherent probe-pump-based Brillouin sensor (or distributed fiber-optic strain and temperature sensor (DSTS)) provides accurate local temperature and strain information at a high spatial resolution by controlling depletion of the pump beam resulting from the strong coherent interaction of the probe and the depleted pump (CIPDP) in the fibers and ensures flat-noise-floor over entire fiber length which offers same resolution and accuracy over entire fiber length and makes simultaneous measurement of strain and temperature possible.

In this work we report bending stress monitoring of an 11km pipeline located in northern Alberta, Canada using temperature compensated distributed fiber-optic strain sensor with CIPDP technique. The results showed that some parts of the pipeline experienced 3,063με during winter from November 2022 when the pipeline was installed to April 2023 when the soil was still frozen. The pipeline leaks due to the ambient temperature change are presented also. The leak volume of 2.187gal with the injection pressure of 105psi and the temperature difference of 39°F (21.6°C) between the line temperature and the soil temperature has been detected in one minute after a leak occurred through 1/8" orifice. All leaks with different volumes controlled by injection pressure, orifice, line temperature, and duration have been detected successfully.

2. Monitoring of bending stress on pipe

2.1 Principle of temperature compensated distributed fiber-optic strain sensor

From Eqs. 1 and 2, it can be concluded that to have strain measurement temperature must be constant (Eq. 1) and to have temperature measurement strain must be constant (Eq. 2). In real application strain and temperature may change simultaneously, represented as

$$\nu_B(T,\varepsilon) = C_\varepsilon(\varepsilon - \varepsilon_0) + C_T(T - T_0) + \nu_{B0}(T_0,\varepsilon_0) \tag{3}$$

thus, the simultaneous measurement of temperature and strain is not directly possible for usual Brillouin scattering-based sensors with a single mode fiber (SMF) since the Brillouin spectrum has only one peak whose frequency is sensitive to both temperature and strain variations. Simply neglecting the effect of temperature will lead to substantial errors in the strain measurements for field applications, as strain changes in structures are usually small (< 100 με) [10]. To solve this problem a second fiber can be placed beside the first fiber and these two fibers with different strain coefficient C_ε and different temperature coefficient C_T are connected in series, in this way the Brillouin frequency shifts $\nu_B^{\mathrm{pk}1}$ and $\nu_B^{\mathrm{pk}2}$ from the 1st and 2nd fiber relating to strain ε and temperature T are given as:

$$\begin{bmatrix} \nu_B^{pk1} \\ \nu_B^{pk2} \end{bmatrix} = \begin{bmatrix} C_\varepsilon^{pk1}(T) & C_T^{pk1}(\varepsilon) \\ C_\varepsilon^{pk2}(T) & C_T^{pk2}(\varepsilon) \end{bmatrix} \begin{bmatrix} \Delta\varepsilon \\ \Delta T \end{bmatrix}, \tag{4}$$

where $\Delta\nu_B^{\mathrm{pk}1(2)} = \nu_B^{\mathrm{pk}1(2)}(\varepsilon,T) - \nu_{B0}^{\mathrm{pk}1(2)}(\varepsilon_0,T_0)$, $\Delta\varepsilon = \varepsilon - \varepsilon_0$, $\Delta T = T - T_0$, ε_0 and T_0 are the strain and temperature corresponding to a reference Brillouin frequency $\nu_{B0}^{\mathrm{pk}1(2)}(\varepsilon_0,T_0)$. If the strain coefficients $C_\varepsilon^{\mathrm{pk}1}(T)$ and $C_\varepsilon^{\mathrm{pk}2}(T)$ and temperature coefficients $C_T^{\mathrm{pk}1}(\varepsilon)$ and $C_T^{\mathrm{pk}2}(\varepsilon)$ for peaks from the 1st fiber and 2nd fiber, respectively, satisfy

$$\begin{vmatrix} C_{\varepsilon}^{pk1}(T) & C_{T}^{pk1}(\varepsilon) \\ C_{\varepsilon}^{pk2}(T) & C_{T}^{pk2}(\varepsilon) \end{vmatrix} \neq 0 \tag{5}$$

the change in strain $\Delta\varepsilon = \varepsilon - \varepsilon_0$ and the change in temperature $\Delta T = T - T_0$ can be obtained.

2.2 Flat-noise-floor over entire fiber length by CIPDP technique

However, it is common sense that the attenuation of fibers increases with the fiber length which causes the performance (i.e. the resolution and accuracy of strain and temperature) of fiber-optic sensors decreases with the fiber length shown in Figure 1. Therefore, Eq. 4 does not give the correct solution of simultaneous measurement of strain and temperature. This is not a theoretical error, but a result of poor performance of fiber-optic sensors.

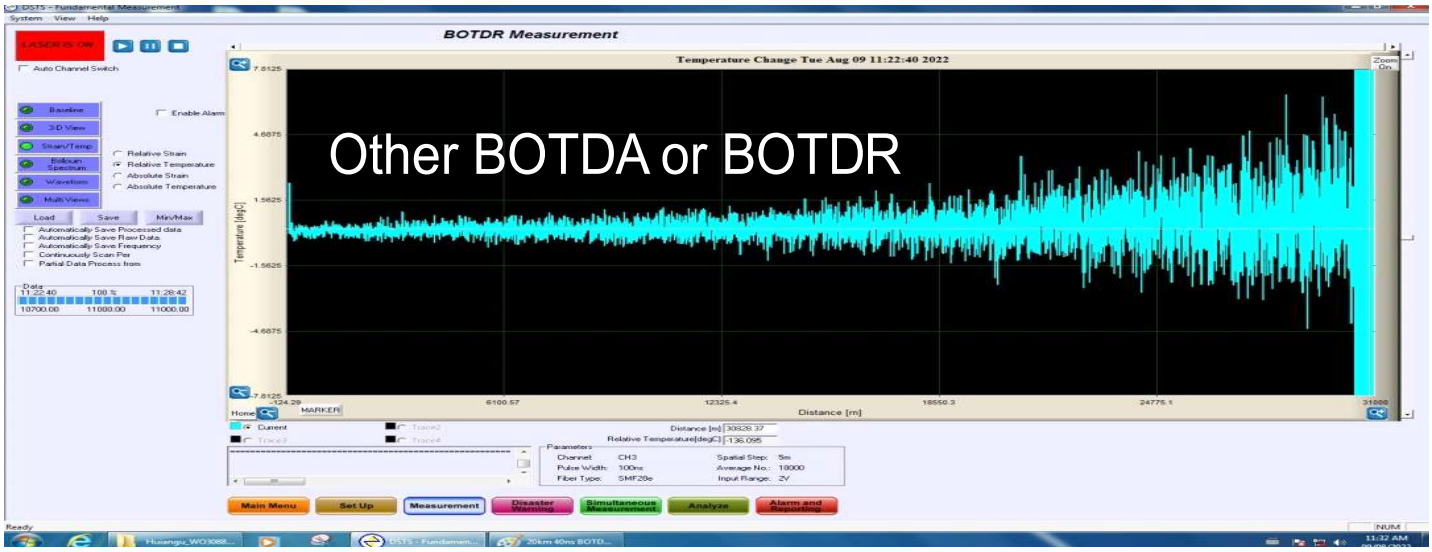

Fig. 1. Poor performance of fiber-optic sensors due to the attenuation of fibers increasing with fiber length.

We have developed a distributed fiber-optic strain and temperature sensor (DSTS) with less than 1mW (Laser Class 1M) of pump power by controlling depletion of pump beam resulting from coherent interaction of probe and depleted pump (CIPDP). DSTS with CIPDP technique ensures flat-noise-floor over entire fiber length shown in Figure 2, which offers same resolution and accuracy over entire fiber length and makes simultaneous measurement of strain and temperature possible.

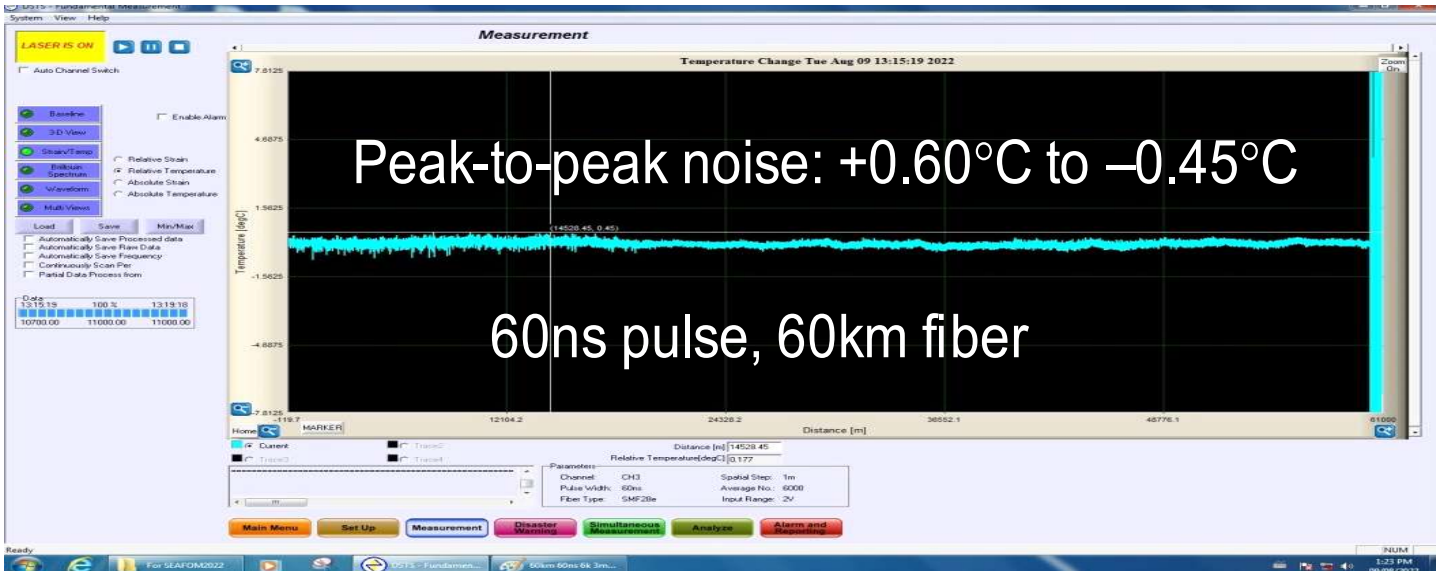

Fig. 2. DSTS with CIPDP technique ensures flat-noise-floor over entire fiber length.

2.3 Installation of optical cables on pipeline and measuring results of baseline

Bending stress on pipes poses a threat to pipeline integrity as it can cause excessive pipe strain, pipe buckling, and severe pipe wall deformation, which can happen before pipeline leakage. Because of environment temperature change, to avoid strain results on pipeline

affected by temperature, a temperature compensated distributed fiber-optic strain sensor with CIPDP technique has been applied for bending stress monitoring of a pipeline located in northern Alberta, Canada. The length of the pipeline is 11 km. To achieve both leakage detection by monitoring temperature and pipeline bending stress by monitoring strain, loosed optical cable and tight-buffer optical cable were connected together and installed on the pipe shown in Figure 3. Thus, the total length of optical fiber is over 22km.

Fig. 3. Loosed optical cable and tight-buffer optical cable were connected together and installed on the pipe.

The Brillouin frequency shifts from entire optical fibers is displayed in Figure 4, and the loosed and tight-buffer optical cables has been connected at 11,743.10m shown in Figure 5. Because tight-buffer was employed on the optical fiber that has been installed tightly on the pipe for pipe strain monitoring, the Brillouin frequency shifts change a lot compared to that from the loosed-buffer optical cable after 11,743.10m with uniform distribution of Brillouin frequency shifts shown in Figures 4 and 5.

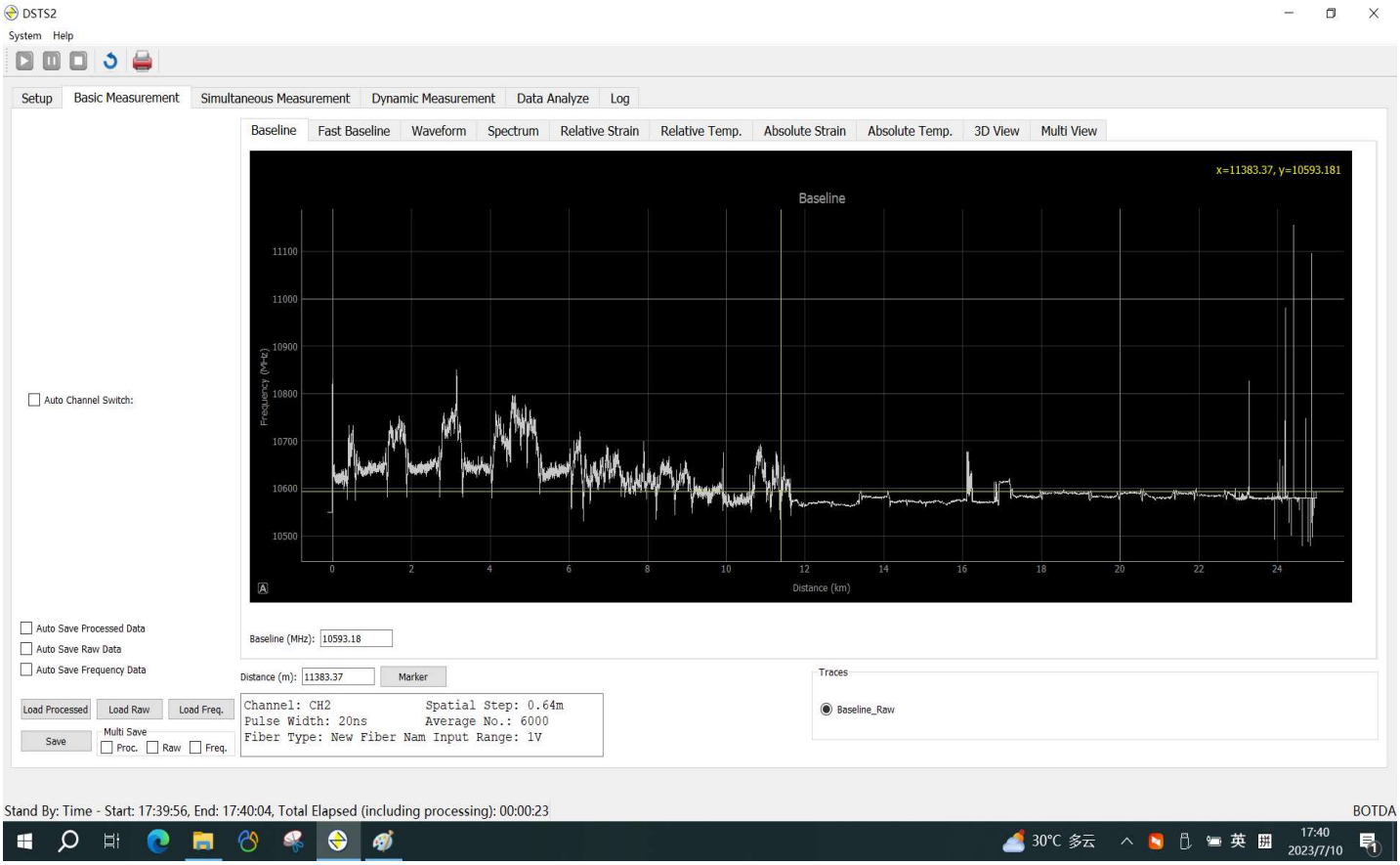

Fig. 4. Brillouin frequency shifts from entire 23,486.20m optical fiber loop including loosed optical cable and tight-buffer optical cable.

Fig. 5. Loosed and tight-buffer optical cables were connected at 11,743.10m.

Figures 6 and 7 demonstrate high quality Brillouin spectra at both loosed and tight-buffer optical cables, which ensures high resolution and accuracy of temperature and strain.

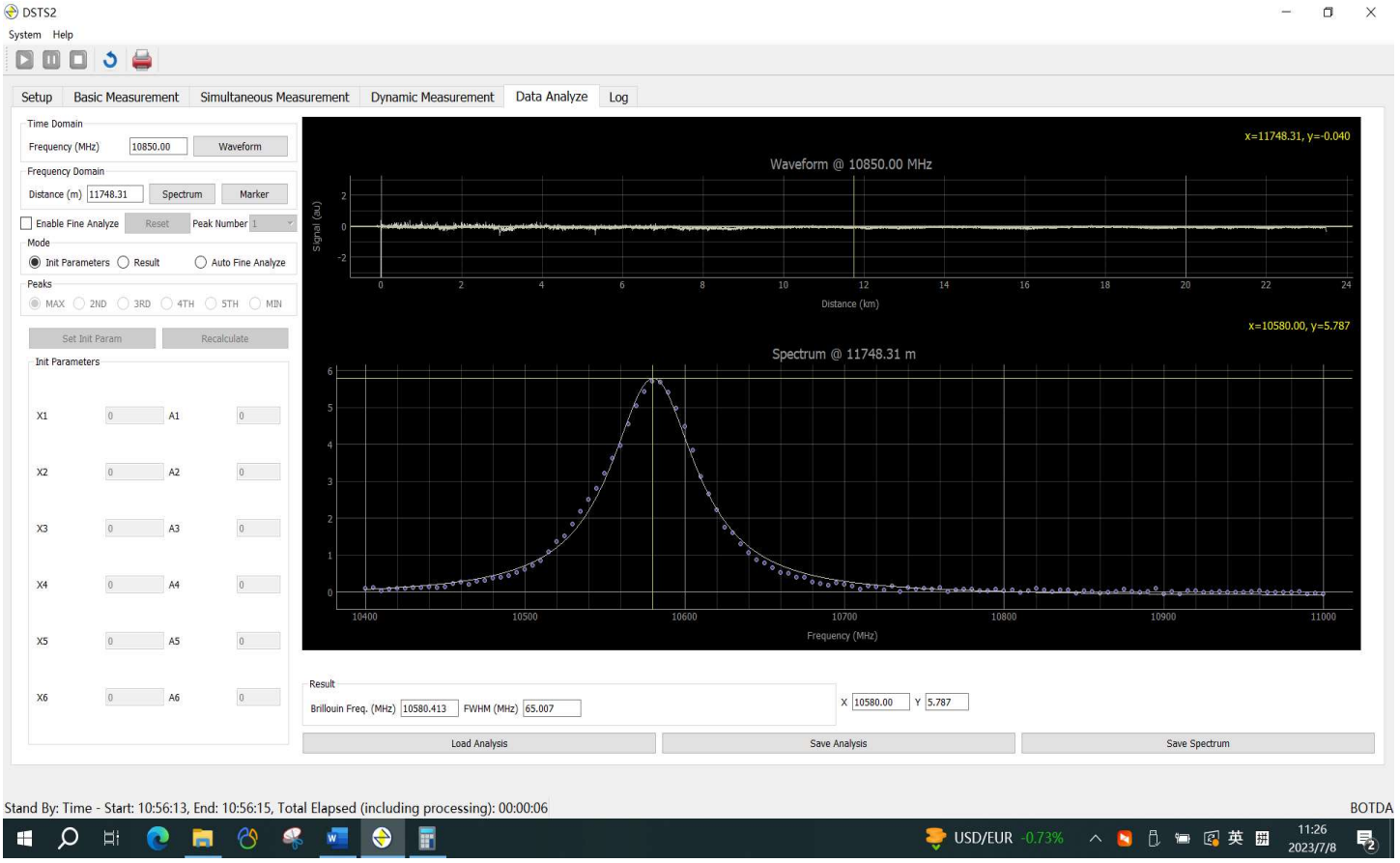

Fig. 6. Brillouin spectrum at 11,748.31m of loosed optical cable.

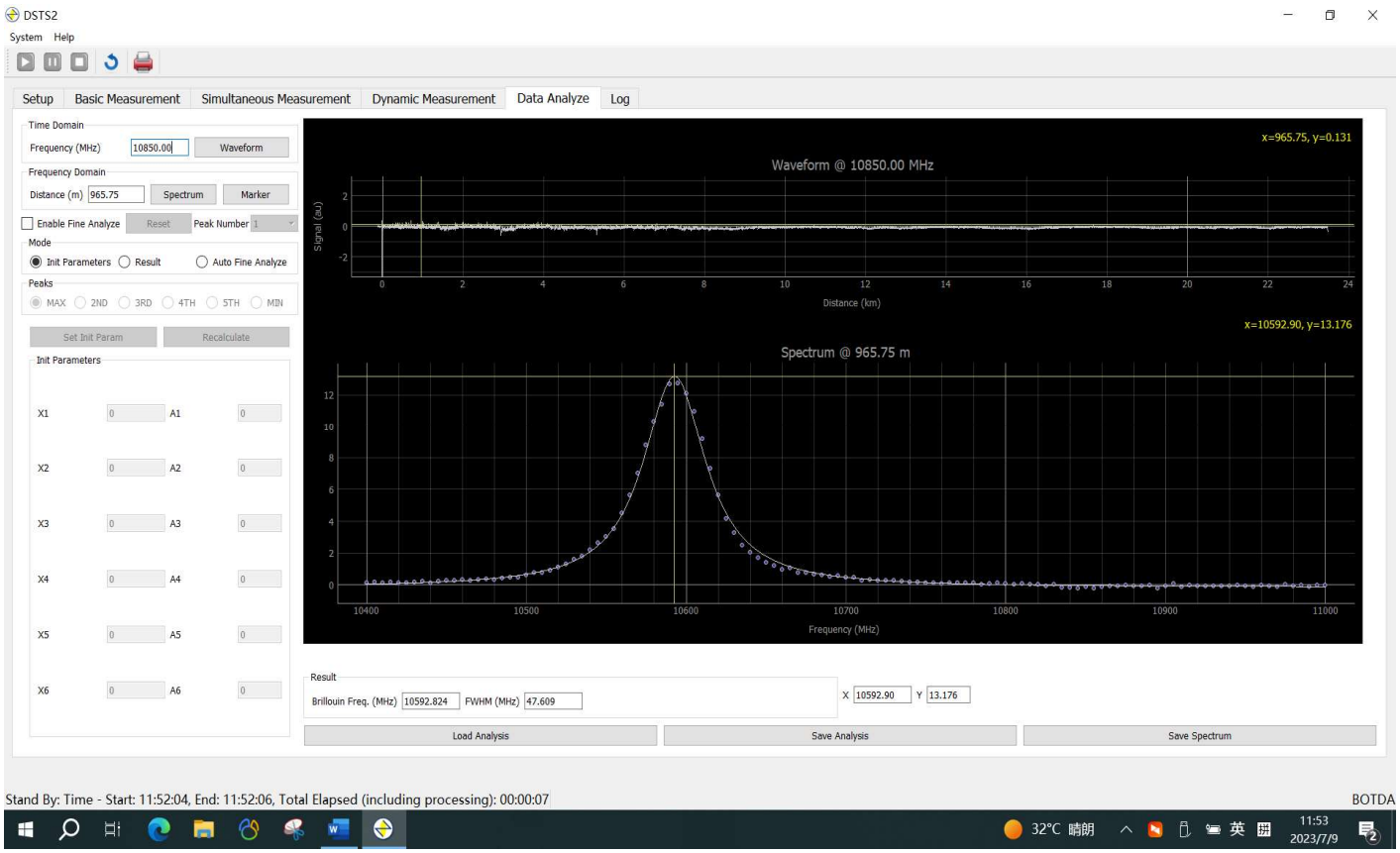

Fig. 7. Brillouin spectrum at 965.75m of tight-buffer optical cable.

2.4 Pipe bending stress monitoring

Compared to Figures 8 to 9, some parts of the pipeline (at 7680.19m) experienced 3,063με during winter from November 2022 when the pipeline was installed to April 2023 when the soil was still frozen. We must pay close attention to pipe bending stress monitoring before the disaster.

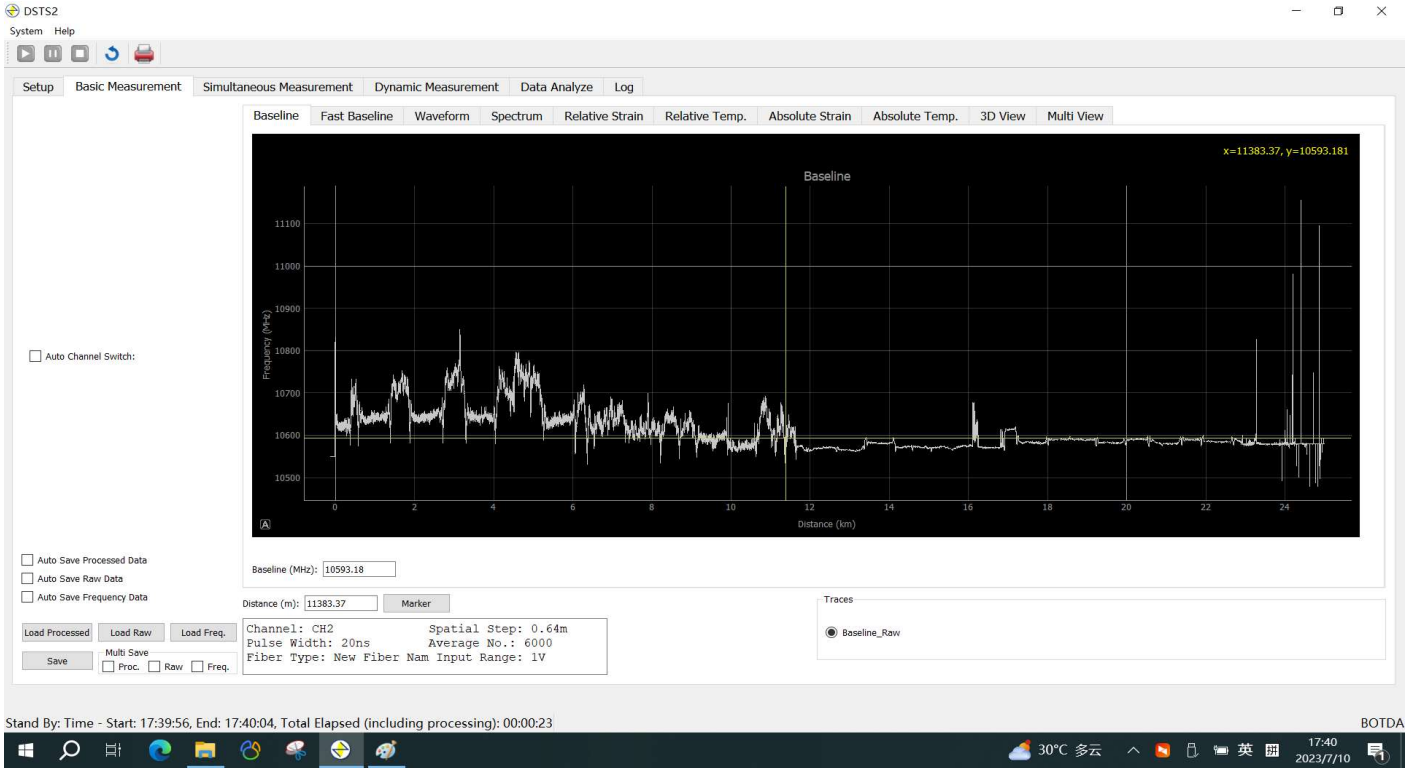

Fig. 8. Brillouin frequency shifts when pipeline was installed on 03 November 2022.

Fig. 9. Pipe experienced 3,063με during winter from November 2022 when the pipeline was installed to April 2023 when the soil was still frozen.

3. Detection of 2.187 gallon pipeline leakage

3.1 Set-up of pipeline leakage tests

Oil and gas pipeline leakage monitoring was carried out at the Southwest Research Institute (SwRI) in San Antonio, Texas [11]. Figure 10 shows a section of the pipeline that was tested, that simulated the leakage of an oil and gas pipeline. Within the pipe, a system of tubing and valves routed the test fluid to the appropriate locations on the pipeline to simulate leaks. The tubing penetrated the pipe wall, and the orifice geometry on the end of the tubing simulated a hole in a pipeline. The orifice discharge was flush with the outside diameter of the pipe. These 3 orifices equipped with electronic control valves could be opened separately or simultaneously to simulate single-hole leakage or multi-hole leakage. The remainder of the pipe was hollow and allowed to fill with water.

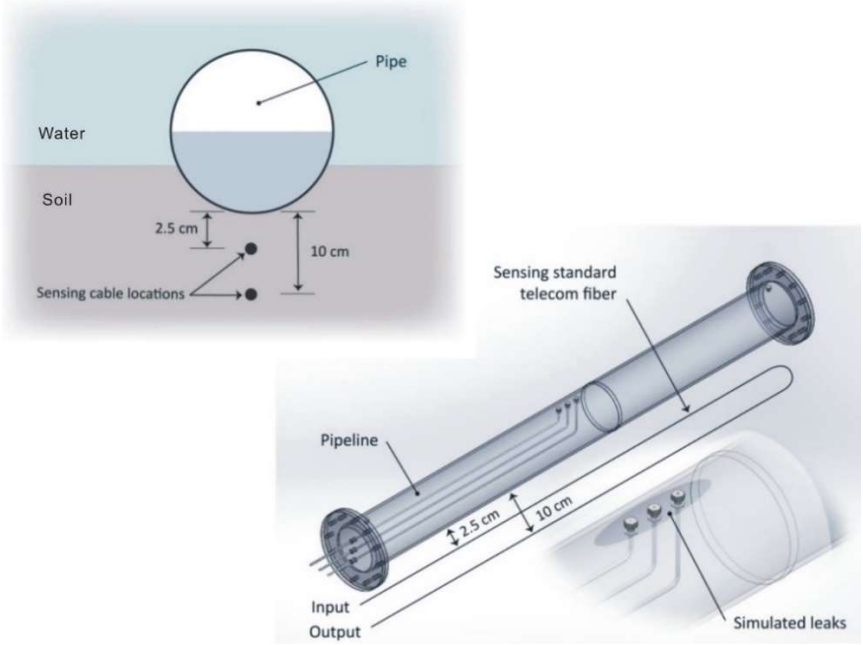

Fig. 10. Schematic diagram of pipeline laying, optical sensing cable laying, and pipeline leak orifices.

A part of the liquid was contained in the pipeline to simulate oil and gas leak. Part of this section of the pipeline was buried in soil, and the rest was covered by water to simulate the actual environment of offshore oil and gas pipelines. The total length of the optical fiber to be tested was 10 kilometers, of which there were two sections of sensing optical cables laid in the soil below the pipeline. One section was located 2.5 cm below the pipeline 6 o'clock, and the other section is located 10 cm below the pipeline 6 o'clock.

Brillouin-scattering-based distributed optical sensors can measure both strain and temperature. If the sensing fiber is loosed, the strain effect can be ignored, and only temperature can be measured. In this test, we used our DSTS based on CIPDP technique with loosed sensing fiber to measure temperature change before and after leaks happen. The spatial information is determined by the analysis of the cw signal in the time domain. A 15 ns pulse duration was used in the measurements to give 1.5 m spatial resolution. Brillouin spectrum measurements were acquired every 4 minutes at a sampling rate of 250 MS/s along the total length of the optical fiber of 10.245 km, using 11,000 averages. The sensor automatically entered the next leak monitoring cycle every 4 minutes. This sensor setting can ensure the measurement accuracy of this sensor is 0.17°C.

3.2 Blind tests of pipeline leakage conducted by SwRI

After the installation of the experimental devices was completed, all sensor manufacturers left from SwRI immediately, and the use of sensors and leakage monitoring were all carried out by technicians from the SwRI. Sensor manufacturers could check the operating status of their sensors through the Internet. The pipeline leak experiments lasted for one and a half months. After the leakage experiments were completed, the sensor manufacturers provided test reports according to the leakage parameters shown in Table 1.

Table 1 Parameters of leakage tests

Date	Start Time	Stop Time	Duration (min)	Orifice	Soil Temp Before Test (F)	Injection Pressure (psi)	Line Temp (F)	Temp Delta (F)
3-Jun	10:26 AM	10:35 AM	09:00.0	1/16"	70	250	95	25.0
4-Jun	11:15 AM	11:25 AM	10:00.0	1/32"	70.5	440	91	20.5
4-Jun	11:37 AM	11:44 PM	07:00.0	1/16"	70.5	385	91	20.5
5-Jun	11:46 AM	11:54 AM	08:00.0	1/8"	85	400	115	30.0
5-Jun	4:12 PM	4:21 PM	09:00.0	1/8"	78	250	119	41.0
6-Jun	1:57 PM	2:10 PM	13:00.0	1/8"	73	105	112	39.0
9-Jun	2:39 PM	2:58 PM	19:00.0	1/8"	70.7	50	113	42.3
10-Jun	2:48 PM	2:58 PM	10:00.0	1/8"	71.5	30	148	76.5
12-Jun	9:06 AM	9:18 AM	12:00.0	1/8"	71	30	105	34.0
12-Jun	10:36 AM	10:49 PM	13:00.0	1/8"	77.5	36	96	18.5
12-Jun	2:40 PM	2:58 PM	18:00.0	1/8"	74	50	95	21.0
13-Jun	10:40 AM	10:50 AM	10:00.0	1/8"	71	38	87	16.0
13-Jun	11:54 AM	12:05 PM	11:00.0	1/8"	73	50	90	17.0
16-Jun	10:26 AM	10:42 AM	16:00.0	1/8"	71	34	87	16.0
16-Jun	11:50 AM	12:09 PM	19:00.0	1/8"	77.5	30	96	18.5
16-Jun	4:16 PM	4:31 PM	15:00.0	1/8"	75	30	103	28.0
17-Jun	10:47 AM	10:56 AM	09:00.0	1/8"	72	150	170	98.0
17-Jun	11:23 AM	11:33 AM	10:00.0	1/8"	72	82	160	88.0
17-Jun	2:38 PM	2:53 PM	15:00.0	1/16"	73	750	150	77.0
23-Jun	10:38 AM	10:48 AM	10:00.0	1/8"	72	52	99	27.0
23-Jun	11:15 AM	11:28 AM	13:00.0	1/8"	72	51	100	28.0
23-Jun	1:54 PM	2:06 PM	12:00.0	1/8"	74	50	101	27.0
23-Jun	2:13 PM	2:25 PM	12:00.0	1/8"	75.5	50	106	30.5
23-Jun	3:23 PM	3:33 PM	10:00.0	1/8"	80	50	105	25.0
23-Jun	3:52 PM	4:05 PM	13:00.0	1/8"	81	51	108	27.0

24-Jun	8:06 AM	8:16 AM	10:00.0	1/8"	73	50	95	22.0
24-Jun	8:22 AM	8:32 AM	10:00.0	1/8"	72	52	94	22.0
24-Jun	9:21 AM	9:33 AM	12:00.0	1/8"	80	40	101	21.0
24-Jun	9:59 AM	10:11 AM	12:00.0	1/8"	79	40	103	24.0
24-Jun	11:37 AM	11:57 AM	20:00.0	1/8"	84	32	105	21.0
24-Jun	1:47 PM	2:08 PM	21:00.0	1/8"	76	31	109	33.0
24-Jun	3:12 PM	3:32 PM	20:00.0	1/8"	88	32	110	22.0
25-Jun	8:55 AM	9:10 AM	15:00.0	1/8"	74	22	94	20.0
25-Jun	10:58 AM	11:15 AM	17:00.0	1/8"	74	40	104	30.0
25-Jun	11:43 AM	11:53 AM	10:00.0	1/8"	76	41	108	32.0
25-Jun	1:31 PM	1:46 PM	15:00.0	1/8"	77	30	107	30.0
25-Jun	2:20 PM	2:33 PM	13:00.0	1/8"	80	21	111	31.0
25-Jun	2:57 PM	3:09 PM	12:00.0	1/8"	85	22	109	24.0
27-Jun	8:00 AM	8:06 AM	06:00.0	1/16"	73	501	159	86.0
27-Jun	10:27 AM	10:32 AM	05:00.0	1/16"	84	405	134	50.0

3.3 Test results of DSTS-based leak detection system (LDS)

When leakage occurs, as long as the temperature of the leakage media is different from the environment temperature, the change of environment temperature due to the leakage can be detected by DSTS. This is the principle behind using DSTS to detect leakage. So, the Brillouin frequencies along the entire fiber must be taken as a baseline. Figure 11 displays the Brillouin baseline frequencies along the entire fiber, taken at 11:02 on June 2nd after the pipe and sensing cable had settled. The sensing cable used for leakage detection was located in the region between 10.044 km and 10.245 km. The Brillouin baseline frequencies from this region were different from the rest of the fiber. For the following leakage tests, this region will be zoomed to display leakage clearly.

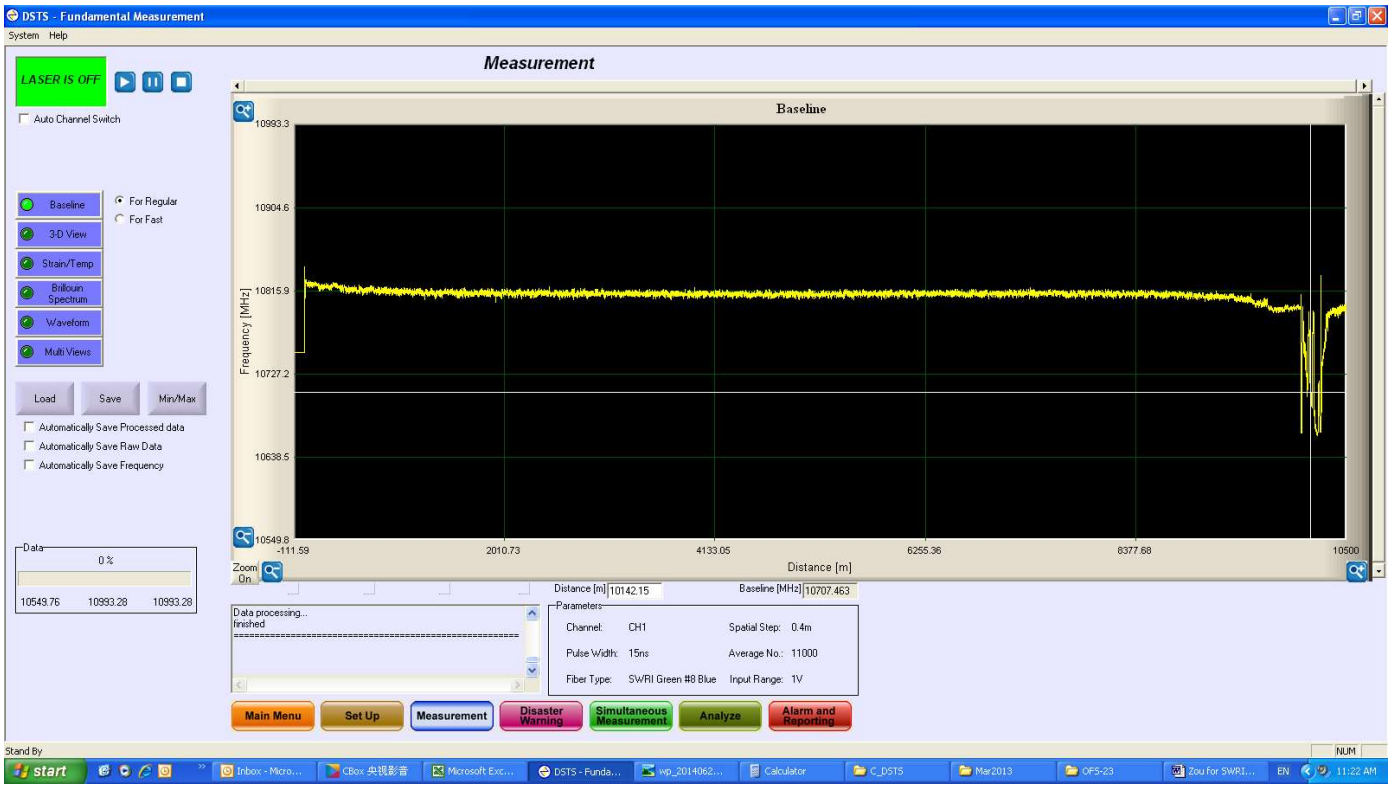

Fig. 11. Brillouin frequencies along 10.245 km as the baseline taken at 11:02 on June 2nd.

The leaks shown in Table 1 were all detected by our DSTS. Due to space limitations, it is impossible to show all the measurement results here. Figures 12 shows one of the results. Readers who need more detailed results can contact the first author, Lufan Zou.

The leaks from the 1/8" orifice started at 13:57, when the injection pressure of the external nitrogen source was 105 psi and the difference between the line temperature and the soil temperature was 39°F (21.6°C).. The red line in Figure 12 is the first measurement result starting at 13:58, which shows that one minute after the leak occurred, the DSTS detected the leakage volume of 2.187 gal through the sensing cable located 2.5 cm below the 6 o'clock point of the pipeline (that is, 10,118.06 m). The temperature change indicated by the red peak here is 1.95°C, which is higher than the intrinsic noise of the positive peak 0.65°C, so it can be affirmed that this is the temperature change peak caused by the leak. However, the temperature change peak through the sensing cable located 10 cm below 6 o'clock of the pipeline (that is, at 10,166.65m) is within the intrinsic noise peak of the DSTS. This would be due to the limitation of the soil's thermal conductivity. The leakage takes a longer time and travels a longer distance to change the soil temperature farther away from the leak orifice. In fact, as the leakage time increases, the volume of leakage increases, which causes the soil temperature around the pipeline leak orifice to increase. Thus, the DSTS detects the leaks through the sensing cables located 2.5 cm (10,118.06 m) and 10 cm (10,166.65 m) below 6 o'clock of the pipeline, as shown by the blue and green lines in Figure 12. The blue line and the green line are the results measured in 5 minutes and 9 minutes after the leak occurred, respectively. The temperature of the green line at the two sensing cables is higher than the temperature of the blue line, which is precisely because the soil temperature around the leak orifices of the pipeline increased with time during 13 minutes of leakage. The difference between the line temperature and the soil temperature was 39°F (21.6°C), but the temperature changes through the sensing cable located 2.5 cm (10,118.06 m) below the 6 o'clock point of the pipeline are 1.95°C, 4.90°C and 6.38°C measured at 1 minute, 5 minutes, and 9 minutes after the leak occurred, respectively. This difference is related to many factors, such as the spatial resolution of the optical sensor, the soil's thermal conductivity, and so on. All these have proposed new research topics for industries related to oil and gas pipelines.

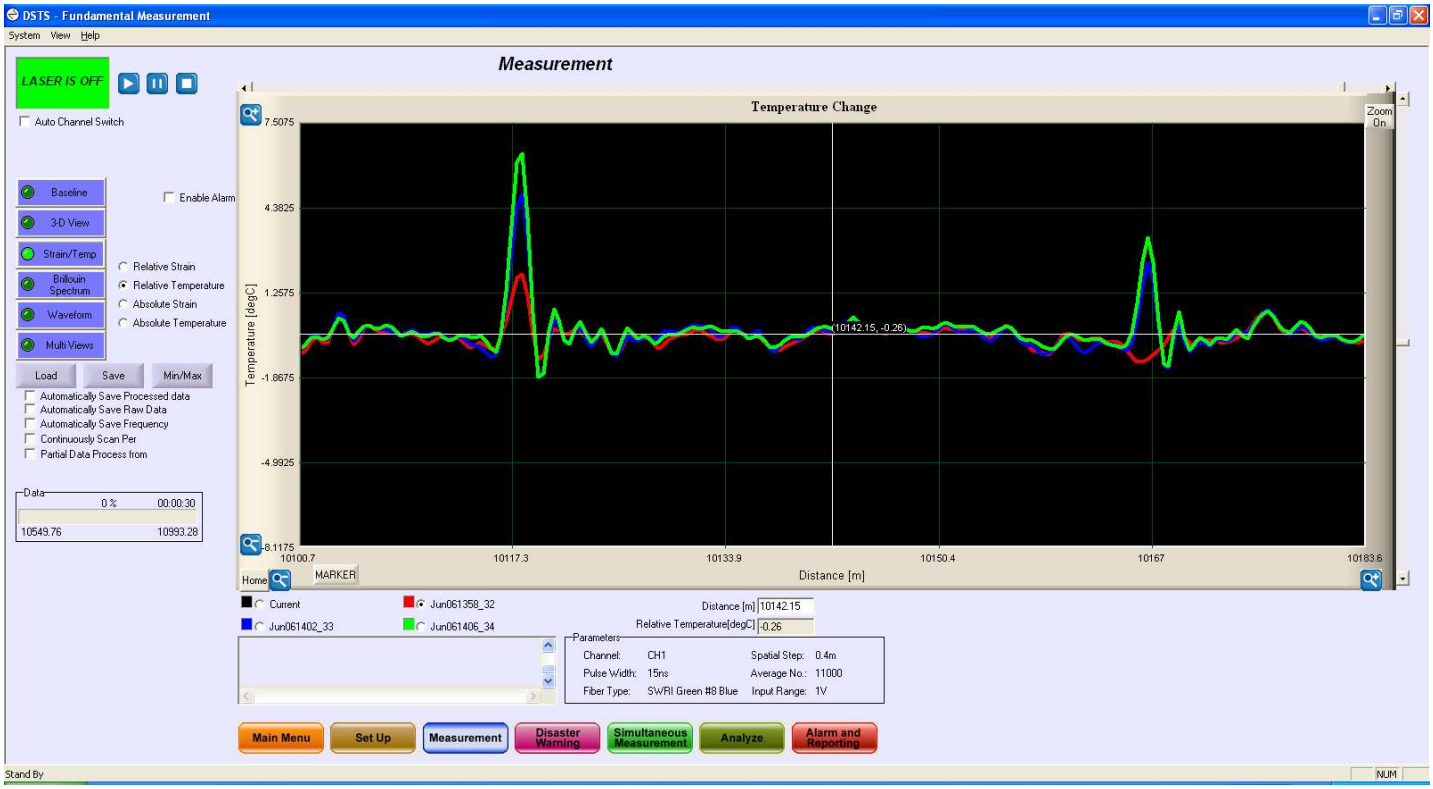

Fig. 12. Leakage volume of 2.187 gal has been detected in 1 minute after a leak happened, shown as the red peak at 10,118.06 m.

4. Conclusions

The bending-stress on an 11km pipeline located in northern Alberta, Canada using temperature compensated distributed fiber-optic strain sensor with CIPDP technique has been reported. The results showed that some parts of the pipeline experienced 3,063με during winter from November 2022 when the pipeline was installed to April 2023 when the soil was still frozen. The pipeline leaks because the ambient temperature changes have been presented also. The leak volume of 2.187gal with the injection pressure of 105psi and the temperature difference of 39°F (21.6°C) between the line temperature and the soil temperature has been detected in one minute after a leak occurred through 1/8" orifice. All leaks with different volumes controlled by injection pressure, orifice, line temperature, and duration have been detected successfully.

References

1. E. Tapanes, "*Fibre optic sensing solutions for real-time pipeline integrity monitoring*," Australian Pipeline Industry Association National Convention, 27-30 October 2001, http://www.iceweb.com.au/Newtech/FFT_Pipeline_Integrity_Paper.pdf.
2. A. Kumar and R. Nickel, "*TC Energy says stress, weld fault caused Keystone oil spill*", 9 February 2023, https://www.reuters.com/business/energy/tc-energy-says-stress-weld-fault-caused-keystone-oil-spill-2023-02-09/.

3. J. Sutton and A. Elamroussi, CNN, "*Last year's Keystone Pipeline shutdown was due to bending stress on a pipe and a weld flaw, company says*", 10 February 2023, https://www.cnn.com/2023/02/10/us/keystone-pipeline-spill-investigation/index.html.
4. L. Zou, X. Bao, Y. Wan, and L. Chen, "*Coherent probe-pump based Brillouin sensor for centimeter-crack detection*," Opt. Lett. **30,** 370–372 (2005).
5. T. Horiguchi, T. Kurashima, and M. Tateda, "*Tensile strain dependence of Brillouin frequency shift in silica optical fibers*," IEEE Photon. Tech. Lett. **1**, 107-108 (1989).
6. T. Kurashima, T. Horiguchi, and M. Tateda, "*Thermal effects on Brillouin frequency shift in jacketed optical silica fibers*," Appl. Opt. **29**, 2219-2222 (1990).
7. X. Bao, D.J. Webb, and D.A. Jackson, "*32-km distributed temperature sensor based on Brillouin loss in an optical fiber*," Opt. Lett. **18**, 1561-1563 (1993).
8. Y. Okawachi, M.S. Bigelow, J.E. Sharping, Z. Zhu, A. Schweinsberg, D.J. Gauthier, R.W. Boyd, and A.L. Gaeta, "*Tunable all-optical delays via Brillouin slow light in an optical fiber*," Phys. Rev. Lett. **94**, 153902-153905 (2005).
9. L. Zou, X. Bao, S. Yang, L. Chen, and F. Ravet "*Effect of Brillouin slow light on distributed Brillouin fiber sensors*," Opt. Lett. **31**, 2698-2700 (2006).
10. L. Zou, G.A. Ferrier, S. Afshar V., Q. Yu, L. Chen, and X. Bao, "*Distributed Brillouin scattering sensor for discrimination of wall thinning defects in steel pipe under internal pressure*", Appl. Opt. **43**, 1583-1588 (2004).
11. S. P. Siebenaler, "*Offshore leak detection joint industry program*", Southwest Research Institute, 22 April 2015.